ORIGINAL PAPER

Sensitive and selective fluorescence detection of guanosine nucleotides by nanoparticles conjugated with a naphthyridine receptor

Piotr J. Cywinski · Artur J. Moro · Thomas Ritschel · Niko Hildebrandt · Hans-Gerd Löhmannsröben

Abstract Novel fluorescent nanosensors, based on a naphthyridine receptor, have been developed for the detection of guanosine nucleotides, and both their sensitivity and selectivity to various nucleotides were evaluated. The nanosensors were constructed from polystyrene nanoparticles functionalized by (N-(7-((3-aminophenyl)ethynyl)-1,8-naphthyridin-2-yl)acetamide) via carbodiimide ester activation. We show that this naphthyridine nanosensor binds guanosine nucleotides preferentially over adenine, cytosine, and thymidine nucleotides. Upon interaction with nucleotides, the fluorescence of the nanosensor is gradually quenched yielding Stern–Volmer constants in the range of 2.1 to 35.9 mM^{-1}. For all the studied quenchers, limits of detection (LOD) and tolerance levels for the nanosensors were also determined. The lowest (3σ) LOD was found for guanosine 3',5'-cyclic monophosphate (cGMP) and it was as low as 150 ng/ml. In addition, we demonstrated that the spatial arrangement of bound analytes on the nanosensors' surfaces is what is responsible for their selectivity to different guanosine nucleotides. We found a correlation between the changes of the fluorescence signal and the number of phosphate groups of a nucleotide. Results of molecular modeling and ζ-potential measurements confirm that the arrangement of analytes on the surface provides for the selectivity of the nanosensors. These fluorescent nanosensors have the potential to be applied in multi-analyte, array-based detection platforms, as well as in multiplexed microfluidic systems.

Keywords Naphthyridine receptor · cGMP · Base pairing · Nucleotide nanosensor · Fluorescence spectroscopy

P. J. Cywinski (✉) · T. Ritschel · H.-G. Löhmannsröben
Department of Physical Chemistry, Institute of Chemistry,
University of Potsdam,
Karl-Liebknecht-Str. 24-25, Golm,
14476 Potsdam, Germany
e-mail: piotr.cywinski@uni-potsdam.de

A. J. Moro
Institute of Physical Chemistry,
Friedrich-Schiller-University Jena,
Lessingstrasse 10,
07743 Jena, Germany

N. Hildebrandt
Institut d'Electronique Fondamentale, Université Paris-Sud 11,
Bâtiment 220,
91405 Orsay Cedex, France

Introduction

The presence of nucleotides is of paramount importance in many cellular processes and pathways within living organisms [1]. Nucleotides take part in human metabolism as sources of chemical energy, in cellular signaling, where they are secondary messengers, and in enzymatic reactions, as incorporated structures into coenzymes and prosthetic groups. Due to their numerous vital roles nucleotides based on a guanine are of particular significance. cGMP primarily takes part in intracellular activities through phosphodiesterases, cyclic nucleotide-gated channels, cAMP- and cGMP-dependent protein kinases. Inside a living cell, cyclic GMP stimulates a protein kinase, which in turn phosphorylates substrate proteins, thereby altering their activity, before the signal is switched off through the hydrolysis of cyclic GMP to GMP by phosphodiesterase [2]. By influencing enzymes, cGMP regulates ion channel conductance, glycogenolysis, and cellular apoptosis [3]. It also plays a distinct role in processes of learning and memory [4] and other processes

within the central nervous system [5]. The role cyclic nucleotides play in the appearance and detection of diabetes [6], asthma [7], cardiovascular diseases [8], and as anticancer agents [9] is still of scientific interest. The importance of cGMP in human physiology is unquestionable; therefore the design and development of new sensing devices for non-invasive cGMP detection and monitoring would provide valuable tools for clinicians and researchers alike.

In the last decade, optical methods have been widely used for the detection of various nucleotides and nucleosides. However, due to their importance, cyclic GMP and cyclic-AMP were the chosen analytical targets in most cases. Luminescent chemical sensors for these nucleotides include molecular organic and inorganic probes, quantum dots, molecularly imprinted polymers and, in recent years, aptamers. The working principle of nucleotide-targeted probes and sensors is based either on the formation of multiple hydrogen bonds between purine base (guanine or adenine) and the complementary moiety of the fluorophore [10], or cation–anion pairing between positively charged fluorophore and negatively charged phosphate group, or groups, present in a nucleotide [11, 12]. Quantum dots utilized for nucleotide detection are usually functionalized with non-fluorescent receptors sensitive to nucleotides. The interaction of the nucleotide with a non-fluorescent receptor stabilizes the quantum dot sterically, which in turn changes its photophysical state, quenching the fluorescence signal. The combinations of organic probes [13, 14] or quantum dots [15] with molecularly imprinted polymers constitute another approach in nucleotide sensing. Molecularly imprinted polymers are materials providing sites which, as in the case of antibodies, are capable of selectively and specifically recognizing the target molecule. Another recognition approach is the application of aptamers combined with chemoluminescent reagents [16] or fluorescent proteins [17]. As artificial oligonucleotides, aptamers are selected from the wide variety of combinations to yield one configuration with a high affinity to the analyte. Although the aptamers exhibit improved resistance towards pH changes and temperature when compared to natural antibodies, they, however, require complicated preparation methodology and are still relatively fragile when compared to chemical sensors [18].

Due to their ability to form triple or quadruple hydrogen bonds, naphthyridines have attracted considerable interest over the past two decades. They have already been successfully used for the molecular recognition of guanine, tartaric acid, carboxylic acid and amino acids [19–21]. It has been shown that acetoamino naphthyridines bind, via triple hydrogen bonds, with guanine preferentially over other nitrogenous bases of adenine, cytosine, thymine, and uracil. This property has been demonstrated in supramolecular chemistry, HPLC separation, and in molecular sensing and mapping of DNA sequences [22–24]. Organic

nanoparticles based on benzofuran–naphthyridine-linked molecules were developed, and their fluorescence was observed in aqueous media [25].

Here, we report on specific base pairing interactions between a nanoparticle surface and a mononucleotide, which, to the best of our knowledge, has not been presented so far. This approach makes it possible to measure both the fluorescence signal and the degree of the nanoparticle stabilization. To a certain limit, this permits each analyte to be studied bimodally, both by fluorescence and ζ-potential measurements.

Experimental

Chemicals and methods

All the chemicals used for synthesis and spectroscopy were purchased from Sigma-Aldrich (Taufkirchen near Munich, Germany) and used without any further purification. All solvents both for chromatography and spectroscopy, as well as labware, were from Roth (Karlsruhe, Germany). ^{1}H NMR spectra were recorded in deuterized dimethyl sulfoxide (DMSO-d_6) on a Bruker 250 spectrometer. The splitting patterns are designated as follows: s (singlet), d (doublet), t (triplet), quin (quintet), and m (multiplet). Preparative column chromatography was carried out in glass columns of different sizes packed with Merck 60 silica gel (0.035–0.070 mm). Mass spectra were recorded on a MAT SSQ 710 from Finnigan. The fluorescence spectra were recorded on a Fluoromax 3 spectrophotometer (Jobin Yvon). For the purposes of time-resolved fluorescence spectroscopy, the frequency tripled output (third harmonic generation) of a Titan Sapphire Laser (Tsunami 3960; Spectra Physics) was used to excite samples. The luminescence was detected in a right angle configuration to the incoming beam. A multi-channel plate (ELD EM1-132/300; Europhoton GmbH) coupled to a FL920 fluorescence lifetime spectrometer (Edinburgh Instruments) was used for the signal detection. The time-resolved emission was collected in the time-correlated single photon counting mode. All luminescence measurements were done at a temperature of $(25\pm1)°C$.

Synthesis of the naphthyridine receptor— (N-(7-((3-aminophenyl)ethynyl)-1,8-naphthyridin-2-yl) acetamide) [20]

In a 25-ml round-bottom flask, 310 mg of 2-acetamido-7-chloro-1,8-naphthyridine (1.4 mmol) (1), 35 mg of PdCl$_2$(PPh$_3$)$_2$ (cat.) and 7.8 mg of CuI (cat.) were stirred in 10 ml of dry THF under argon. To the solution, 2 ml of triethylamine was slowly added through a syringe. The mixture was stirred at room temperature for 30 min and then 0.2 ml of 3-ethynylaniline (1.9 mmol) (2) were added drop-

wise. The reaction was stirred at room temperature overnight. Upon removal of the volatiles under reduced pressure, the residue was dissolved in dichloromethane, passed through a plug of celite and then washed with ethyl acetate. The solvents were removed under reduced pressure and the crude product was dried under vacuum. Column chromatography in silica gel with an increasing gradient of methanol in dichloromethane (DCM/MeOH from 20:1 to 10:1) yielded 180 mg of pure (N-(7-((3-aminophenyl)ethynyl)-1,8-naphthyridin-2-yl) acetamide) (3) (η=43%). Spectral data: ^{1}H NMR (400 MHz, DMSO-d$_6$): δ 11.02 (s, 1H, NH amide); 8.43 (m, 3H); 7.65 (m, 1H); 7.11 (t, 1H, J=7,8 Hz); 6.84 (s, 1H); 6.79 (d, 1H, J=7,8 Hz); 6.69 (d, 1H, J=7,8 Hz); 5.32 (s, 2H, NH$_2$); 2.20 (s, 3H, CH$_3$). ^{13}C NMR (100 MHz, DMSO-d$_6$) δ 170.8, 155.4, 155.1, 149.4, 146.3, 139.7, 138.0, 129.9, 124.2, 121.7, 119.8, 116.9, 116.1, 115.7, 91.8, 88.8, 24.7. EI-MS (m/z) 302.3 (for mass spectra see electronic supplementary information). Spectral characteristics: absorbance maxima: λ_1= 300 nm, λ_2=370 nm; Fluorescence λ_{em}=530 nm. The maximum of the fluorescence excitation spectrum overlaps with the absorbance maxima. The fluorescence lifetime was measured to be τ_f=3.4 ns.

Synthesis of the nanosensors

A volume of 0.5 ml of an aqueous suspension of latex beads (2.65% solid latex) with carboxylic acid on the surface (Polybead®, 50 nm, Polysciences, Inc., Warrington, PA, USA) were dispersed in 5 ml of MES 50 mM (pH 6). Then, 0.56 mg of N-(3-dimethylaminopropyl)-N-ethylcarbodiimide hydrochloride, and 0.59 mg of N-hydroxysulfosuccinimide was then added and left to react for 15 min at room temperature. Then, this suspension was washed twice in MES and concentrated by ultrafilters (100 kD molecular weight cut off, Millipore). The resulting suspension was re-dispersed in 5 ml of MES solution, and 2.2 mg of the receptor molecule in ethanol was then added. The suspension was left to react for 2 h. Then the samples were washed in MES buffer containing 100 mM ethanolamine. Finally, the nanosensors were multiply washed (up to eight times) with 10 ml of MES/ethanol (4:1) and twice with pure MES buffer and concentrated to 2 ml to be used for further analysis. Spectral characteristics: λ_{1abs}=300 nm, λ_{1abs}=360 nm, λ_{em}=520 nm, τ_f=1.2 ns (for Raman spectra of pure and conjugated particles see electronic supplementary information).

For fluorescence spectroscopy, an aliquot (100 μL) of this final dispersion was diluted in 5 ml of HEPES buffer 0.1 M at pH 7.4 (OD≤0.2) and 3 ml of this solution was transferred to a 1×1 cm quartz cuvette (Hellma GmbH). Small aliquots (20 μl the smallest) of the analyte 1 mM solution (up to a total volume of 300 μL) were then added to the cuvette to study the influence of the nanosensor's fluorescence. The pH value remained constant throughout all the measurements, as measured using a pH meter (Hanna Instruments, Woonsocket, MI, USA).

Synthesis of reference nanoparticles

A volume of 0.5 ml of an aqueous suspension of latex beads (2.65% solid latex) with carboxylic acid on the surface (Polybead®, 50 nm, Polysciences, Inc., Warrington, PA, USA) was dispersed in 5 ml of MES 50 mM (pH 6). Then 0.1 mg of methacryloxethyl thiocarbonyl rhodamine B (PolyFluorTM 570, Polysciences, Inc., Warrington, PA, USA) in 2 ml ethanol was added and the solution was stirred for 1 h at room temperature. The nanoparticles were then exposed to UV irradiation (λ_{max}= 312 nm) for 15 min, multiply washed (up to 10 times) in MES/ethanol (4:1) and twice with pure MES, each time concentrated by ultrafilters, and the resulting suspension re-dispersed in 5 ml of MES solution. Finally, an aliquot (100 μL) of this solution was dispersed in 5 ml of HEPES buffer 0.1 M at pH 7.4 (OD≤ 0.2) and then 0.5 ml of this solution was transferred to a 1× 1 cm quartz cuvette (Hellma GmbH, Jena, Germany) containing the nanosensor suspension.

Electronic structure calculations

Quantum mechanical DFT calculations were carried out at the B3LYP/6–31+G* level using the Gaussian 09 software package [26, 27]. The influence of the solvent (H$_2$O) was taken into account by the polarizable continuum model (PCM) [28] in its integral equation formalism variant (IEFPCM) as devised by Tomasi and coworkers [27, 29]. The geometric structures were fully optimized at the PCM level and vibrational frequencies were calculated to confirm the absence of imaginary frequencies. Molecular volumes, defined by the volume inside a 0.001 electrons/bohr^3 [30] density envelope, were computed by Monte-Carlo integration as implemented in the Gaussian.

ζ-potential measurements

The change of the ζ-potential of the fluorescent nanosensors in the presence of nucleotides was measured with a Zetasizer Nano Zs (Malvern instruments GmbH, Herrenberg, Germany) equipped with an MPT-2 titrator. An aqueous suspension of the nanosensors was filtered through a 0.45 μm PTFE membrane before measurement. A constant value of pH=7.4 was maintained and controlled throughout the whole experiment.

Results and discussion

The principle of molecular recognition of cGMP is based on mimicking the interactions that occur between nucleotide

bases naturally (Scheme 1). The hydrogen bonding is mimicked by the naphthyridine present on a nanoparticle surface and the cGMP. The stabilization of the colloidal naphthyridine functionalized nanoparticle by the negatively
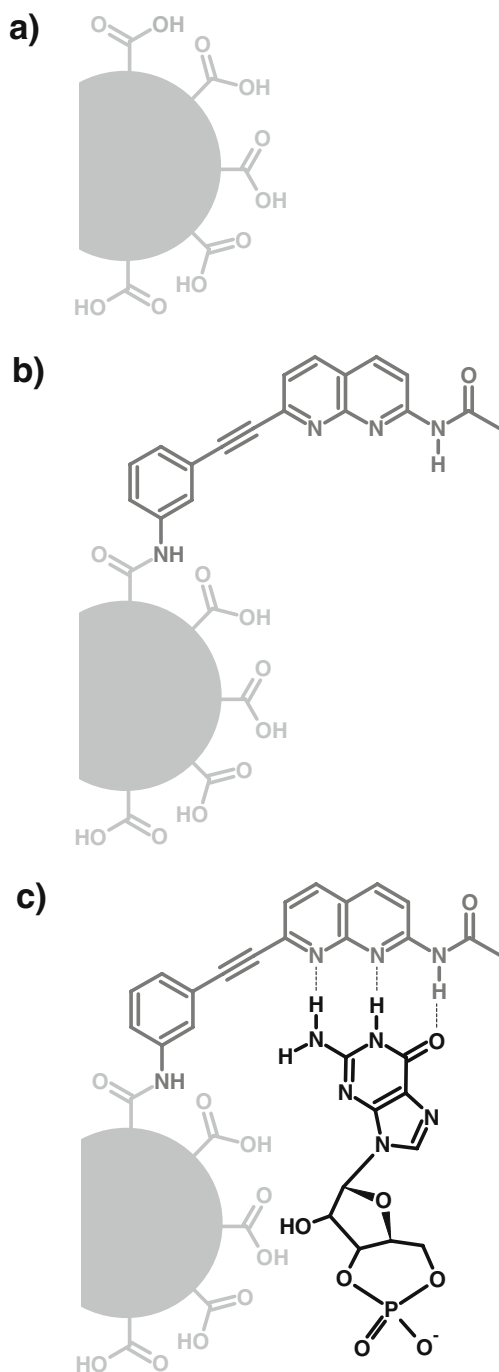
Scheme 1 Scheme of the architecture and operational principle of the nanosensor. **a** Starting material with carboxylic groups on the surface; **b** fluorescent nanosensor with naphthyridine coupled to the surface; and **c** proposed principle of the nucleotide recognition and nanoparticle stabilization caused by the presence of the negatively charged phosphate group

charged phosphates of the nucleotides can be considered the second phenomenon taking part in the recognition process. The principle of recognition can be described as follows: initially the nanoparticle suspension is stable because of the presence of carboxylic groups (Scheme 1a). After the carbodiimide-driven functionalization, the surface loses a major part of its charge due to the coupling of the naphthyridine (Scheme 1b). This conjugation leads to the introduction of a fluorescent moiety to the nanoparticle and to decreased stability. When the fluorescent nanosensor then comes in contact with guanosine nucleotides, the stability is restored (Scheme 1c). This can be observed by the fluorescence quenching as a consequence of electron transfer from the quencher to the nanosensor. Independently, this phenomenon is also observed by measuring the ζ-potential at the surface of the nanoparticles. The ζ-potential changes from -80 mV, in the case of carboxylic functionalized nanoparticles (Scheme 1a), to -32 mV for naphthyridine functionalized NPs (Scheme 1b), and then decreases to -39 mV at 100 μM of cGMP concentration (Scheme 1c). When this happens, the nucleotides play the role of a dispersant (stabilizer). Nanoparticles are commonly stabilized by non-specific adsorption of a dispersant layer around the particle surface. The formation of a dispersant layer of appropriate thickness is crucial for the stabilization of suspensions. In our case, the dispersant layer is composed of guanosine moieties located immediately adjacent to the nanoparticle surface, which provide Coulombic repulsion, and the phosphate groups have counter anions to provide the charge balance. These guanosine nucleotides confer the nanoparticle with the ability to balance inter-particle attractive and repulsive forces thus providing colloidal stability. The use of nucleotides or DNA fragments for colloidal non-specific stabilization has been reported previously [31–35]. In the case of gold nanoparticles, the addition of nucleotides or aptamers improved the colloidal stability, and consequently caused a change in the color of the suspension [36, 37]. The influence of nucleotide functionalities on the growth of semiconductor quantum dots has also been studied [38].

Moreover, for fluorescence microscopy investigations in real samples, e.g., living cells or tissues, any unwanted changes in nanosensor fluorescence, due to sudden fluctuations in sensor concentration, or because of shifts in the focal plane of the excitation source, can be corrected by the presence of a reference fluorophore [39–41]. Therefore, to the nanosensor suspension, we introduced nanoparticles containing rhodamine, which is not itself responsive to the cGMP. The reference particles had only carboxylic moieties on their surfaces, and are assumed to be incapable of nucleotide binding. Having a reference sensor as a completely different particle reduces the chances of any unwanted Förster resonance energy transfer, which could occur if the reference sensor were on the same particle [42].

Nevertheless, we calculated the Förster radius for our system according to the formula:

$$R_0^6 = 8.79 \cdot 10^{-5} \left(\kappa^2 n^{-4} \Phi_0 J(\lambda) \right) \qquad (1)$$

where κ^2 is the dipole orientation factor, n is the refractive index of water, Φ_0 is the fluorescence quantum yield of the donor in the absence of the acceptor, and J is the spectral overlap between donor fluorescence and acceptor absorbance (in M^{-1} cm^{-1} $(nm)^4$). With the use of this formula, we found the Förster radius to be equal to 3 nm. Although there is an overlap of the fluorescence emission of the nanosensors with the absorbance of the rhodamine present in the reference nanoparticles, no energy transfer was observed. This is likely due to the low probability of permanent positioning of the two dyes at the distance of 3 nm.

Fluorescence spectra of the nanosensors and gradual quenching with increased concentrations of cGMP are shown in Fig. 1.

A decrease of the nanosensor fluorescence (around fivefold) is observed upon the addition of up to 100 μM cGMP, whereas the fluorescence of the reference nanoparticles is essentially unaffected. The quenching is most likely due to electron transfer from the guanosine nucleotides to the naphthyridine moiety enabled by the triple hydrogen bonding (Scheme 1c). The fluorescence lifetime of the nanosensor is unchanged over the complete cGMP concentration range. This gives very good evidence that the fluorescence quenching is of static character caused by the formation of a stable nanosensor–analyte complex in the ground state [43].

To study the selectivity of our nanosensor, we chose a variety of nucleotides, which can be divided into two groups. The first consists of cyclic mononucleotides with different purine and pyrimidine bases (cAMP, cCMP, and cTMP) and the second is composed of guanosine nucleotides with varying numbers of phosphate groups (GTP, GDP, and

Fig. 1 Quenching of the nanosensor fluorescence with increasing concentrations of cGMP in 0.1 M HEPES buffer pH 7.4 (λ_{exc}= 350 nm). The reference signal stays essentially unaffected (λ_{exc}= 514 nm)

GMP). The second group was chosen to test our nanosensors in order to determine the influence of the number of phosphate groups on colloidal stability, and to subsequently determine the stability vs. fluorescence of the nanosensors. Chemical structures of analytes used in this study are shown in Table 1.

The rationale behind this choice is based on the fact that all of the studied nucleotides are found within living cells and can be considered main interferents of the analytical signal. Results show a quenching tendency directly proportional to the concentration of all the studied guanine nucleotides, with virtually no quenching from other mononucleotide analytes. To distinguish between the guanosine nucleotides, we described their fluorescence quenching by the use of Stern–Volmer (S–V) plots (Fig. 2a) and the S–V constants according to the equation as follows:

$$\frac{\int_{\lambda=450nm}^{\lambda=550nm} I_0(\lambda)d\lambda}{\int_{\lambda=450nm}^{\lambda=550nm} I(\lambda)d\lambda} = 1 + K_{SV}[Q] \qquad (2)$$

where I_0, I is fluorescence intensity in the absence and in the presence of the quencher, respectively. K_{SV} is the Stern–Volmer constant, and Q represents concentration of a quencher.

The S–V constants for all the analytes studied are presented in Table 2. The magnitude of the quenching constants depends on the base present in each of the cyclic nucleotides (cGMP>>cTMP>cCMP>cAMP) as well as the number of phosphate groups (cGMP>GMP>GDP> GTP). We attribute this specific order for purine bases to the fact that guanine, as the strongest donor amongst them [44], causes the strongest effect on nanosensor fluorescence. The difference in the recognition properties of the nanosensors with regards to the differing number of guanosine phosphate groups in the nucleotide is likely to be due to the space available for binding. Even though the nucleotides are capable of rotating around their glycosidic bonds, the accessibility of the binding site is spatially limited by the charge of the nucleotide. The three phosphate groups of GTP occupy a larger space, and bring more charge to the nanoparticle surface than cGMP possessing only one phosphate group and one negative charge. Since the fluorescence quenching is mostly dependent on the base pairing efficiency, it seems obvious that the presence of fewer guanosine moieties would cause weaker quenching. Although both cGMP and GMP possess one phosphate group, the response is different for each of them. We attribute this feature to the difference in their freedom to move associated with relative structural rigidity (cGMP> GMP).
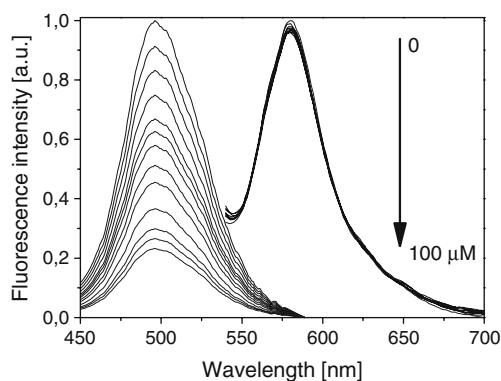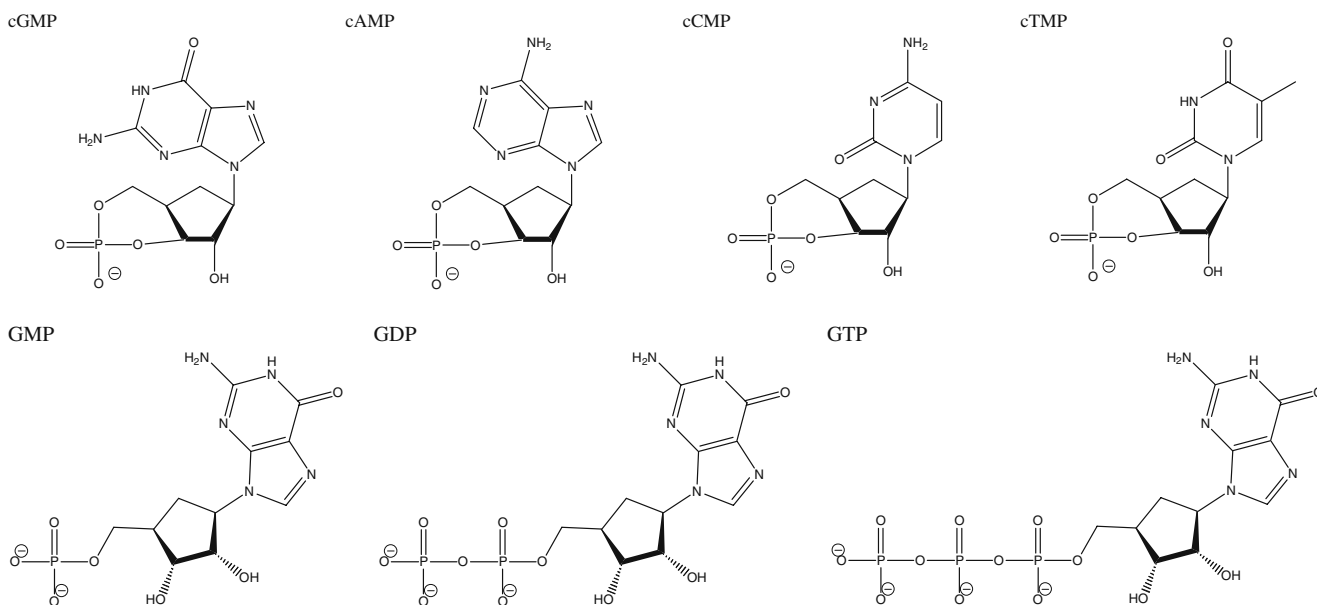
Table 1 Chemical structures of all analytes used in this study

cGMP

cAMP

cCMP

cTMP

GMP

GDP

GTP

Therefore, assuming all possible sites are occupied, the phosphate groups will form a shell around the nanoparticle. Since the number of groups which are required to cause stabilization is essentially constant, fluorescence quenching is only dependent on the number of guanosine moieties available for binding. To support this assumption, we performed molecular modeling on the volumes of the complexes formed between naphthyridine and each of the guanosine nucleotides. The volumes are also given in Table 2. The results show that the volume of the complex increases as the number of phosphate groups increases, which, in turn, limits the space available for binding on the nanoparticle surface. Additionally, to support the aforementioned considerations we performed a set of ζ-potential measurements on the nanosensors in the presence of each of guanosine nucleotides (pH 7.4). The ζ-potential vs. nucleotide concentration for each guanosine nucleotide is shown in Fig. 3. One can observe that, in the case of cGMP, the ζ-potential constantly decreased over the whole range of studied concentrations. For the other nucleotides, it was possible to distinguish two characteristic behaviors. The first is a relatively steep decrease in the concentration range where a nucleotide actually interacts with the nanoparticle surface (between 0 and ca. 20 μM). The second is described by a plateau as a consequence of the lack of this interaction due to lack of space available for binding. The steepness of ζ-potential slope increased in the following order: cGMP/GMP/GDP/GTP, which is associated with the number of phosphate groups and negative charges. The steepness values are also presented in Table 2.

In order to verify the sensitivity and selectivity of our nanosensor, we separately determined the limits of detection (LODs) and tolerance levels (TL) for each of the studied guanosine nucleotides. The limits of detection for each of the studied quenchers were calculated using the following equation:

$$LOD = \frac{3\sigma}{a} \qquad (3)$$

where σ is the standard deviation of the fluorescence signal in the absence of a quencher calculated from 2,000 experimental points, and a is the slope of the linear dependence (at low cGMP concentration) of fluorescence intensity vs. quencher concentration. The tolerance limits for each of the fluorosensors were calculated on the basis of a systematic study of the quenching effects of the drugs, in buffer, in the presence of 0.1 mM. The concomitant species were tested at different concentration levels, and, if interference occurred, the concentration of these species was reduced until the result was included in the confidence interval defined as significant by Student's t test statistics ($P < 0.05$).

Both the LODs and TLs of our nanosensors for all the analytes are presented in Table 2. The nanosensor LODs are still slightly above concentrations found in living cells, but, even though one can find molecular systems having LODs in the range of $0.1-0.3 \times 10^{-9}$ M [45], no selectivity towards guanosine nucleotides is introduced to them. The LOD for cGMP was found to be 150 ng/ml, which is still above the concentration of cGMP usually found in human plasma. It is
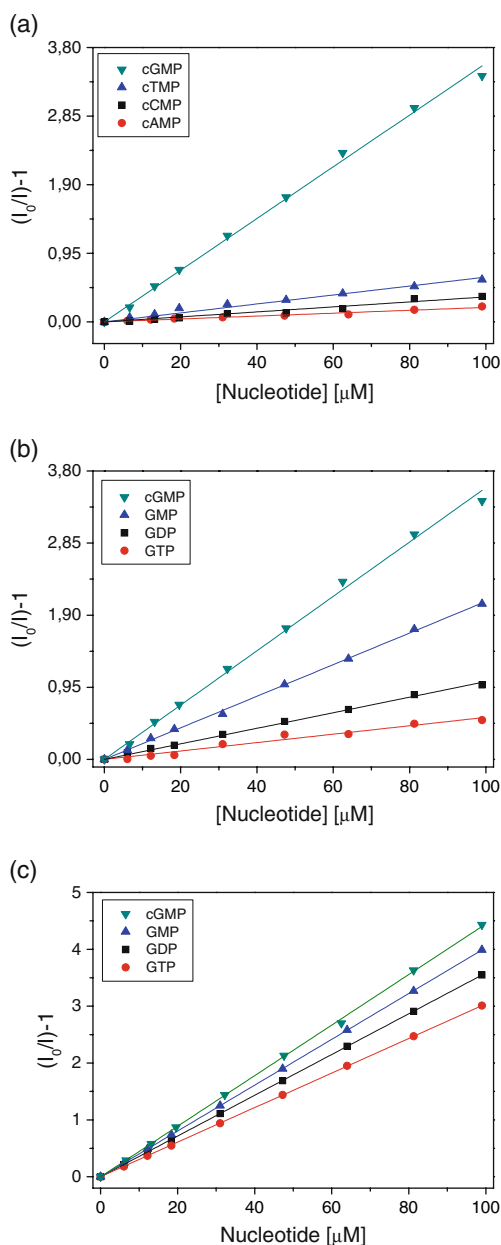
(a)

(b)

(c)

Fig. 2 Stern–Volmer plots for the nanosensors in the presence of various nucleotides obtained from steady-state fluorescence spectroscopy. **a** Cyclic monophosphate nucleotides with different bases; **b** guanosine-based nucleotides with different numbers of phosphate groups; (**c**) the response of free receptor in solution to different guanosine nucleotides

Table 2 Stern–Volmer constants (K_{SV}), limits of detection (LOD), tolerance levels (TL), steepness of ζ-potentials of naphthyridine nanosensors (A) and complex volumes between naphthyridine receptor and each guanosine nucleotide (V_{R-N})

Analyte	K_{SV} [mM^{-1}]	LOD [ng/ml]	TL [mM]	A [mV/µM]	V_{R-N} [Å^3]
cGMP	35.9±0.5	150±5	–	−0.08	675
GMP	20.8±0.3	280±10	0.3	−0.22	738
GDP	10.2±0.2	720±26	1	−0.66	805
GTP	5.5±0.1	1,700±70	2.4	−1.04	845
CTMP	6.2±0.2	1,500±50	2	–	–
cCMP	3.6±0.2	2,600±100	3.6	–	–
cAMP	2.1±0.1	4,450±200	6	–	–

of various guanosines, which can be considered a limitation of the presented approach.

Conclusion

In conclusion, a naphthyridine dye sensitive to guanosine nucleotides was successfully synthesized. On the basis of this dye, fluorescent nanosensors maintaining the ability to recognize guanosine nucleotides were synthesized by carbodiimide-driven esterification. The nanosensors developed produce strong, stable, and highly reproducible fluorescence signals. They are easy to prepare, have LODs for nucleotides between 0.15 and 4.5 µg/ml, and are based on readily available commercial products. The nanosensor exhibits high sensitivity towards guanosine nucleotides, in particular for cGMP and GMP. One major advantage of our nanosensors is the selectivity towards different guanosines, a property that the molecular napthyridine receptor in solution cannot offer. The sensitivity to other cyclic nucleotides was found to be quite low, and independent of the number of
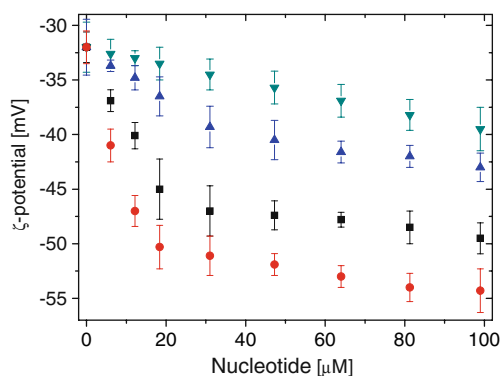
also in the range of the LODs usually found for systems utilizing base pairing as the recognition mechanism [46]. We also tested the nanosensor's ability to detect cGMP from a mixture of different guanosine nucleotides. We titrated cGMP in a solution containing 30 µM of GMP, 20 µM of GDP, and 10 µM of GTP and we still were able to detect cGMP under these conditions. The LOD for cGMP was found to be 300 ng/ml. Noticeably, in real media, the same signal change can be associated with various concentrations

Fig. 3 ζ-potential of napthyridine nanosensors as a function of concentration of guanosine nucleotides: *filled inverse triangle* cGMP, *filled upright triangle* GMP, *filled square* GDP, *filled circle* GTP

phosphate groups. Due to their low limits of detection, presented naphthyridine nanosensors have the potential to be applied to multi-analyte array-based detection platforms, as well as microfluidic systems.

References

1. Kaupp UB, Seifert R (2002) Physiol Rev 82:769–824
2. Robison GA, Butcher RW, Sutherland EW (1971) Cyclic AMP. Academic, New York
3. Beavo JA (1995) Physiol Rev 75:725–748
4. Miyazaki S, Imaizumi M, Abiru T, Machida H (1999) 64:45–52
5. Kurauchi Y, Hisatsune A, Isohama Y, Katsuki H (2009) Neuroscience 158:856–866
6. Yeo JL, Tan BTCh, Achike FI (2010) 642:99–106
7. Giannini L, Nistri S, Mastroianni R, Cinci L, Vannacci A, Mariottini C, Passani MB, Mannaioni PF, Bani D, Masini E (2008) J Cell Mol Med 12:2381–2394
8. Tsai EJ, Kass DA (2009) Pharmacol Ther 122:216–238
9. Browning DD, Kwon I-K, Wang R (2010) Future Med Chem 2:65–80
10. Amemiya S, Buhlmann P, Umezawa Y (1997) Chem Comm 1027–1028
11. Turkewitsch P, Wandelt B, Darling GD, Powel WS (1998) J Photochem PhotoBiol A Chem 117:199–207
12. Wandelt B, Cywinski P, Darling GD, Stranix BR (2005) Biosens Bioelectron 20:1728–1736
13. Cywinski P, Sadowska M, Danel A, Buma WJ, Brouwer AM, Wandelt B (2007) J Appl Polym Sci 105:229–235
14. Cywinski P, Wandelt B, Danel A (2004) Ads Sci Tech 22:719–729
15. Diltemiz SE, Say R, Bueyuektiryaki S, Huer D, Denizli A, Ersoez A (2008) 75:890–896
16. Yan X, Cao Z, Kai M, Lu J (2009) Talanta 79:383–387
17. Platt M, Rowe W, Wedge DC, Kell DB, Knowles J, Day PJR (2009) Anal Biochem 390:203–205
18. Cho EJ, Lee J-W, Ellington AD (2009) Annu Rev Anal Chem 2:241–264
19. Goswami S, Ghosh K, Mukherjee R (2001) Tetrahedron 57:4987–4993
20. Lu S-H, Selvi S, Fang J-M (2007) J Org Chem 72:117–122
21. Yoshimoto K, Atsumi A, Saito S, Okuma M, Maeda M, Nagasaki Y (2007) Nucleic Acids Symp Ser 51:303–304
22. Corbin PS, Zimmerman SC, Thiessen PA, Hawryluk NA, Murray TJ (2001) J Am Chem Soc 123:10475–10488
23. Feibush B, Saha M, Onan K, Karger B, Giese R (1987) J Am Chem Soc 109:7531–7533
24. Nakatani K, Sando S, Saito I (2000) J Am Chem Soc 122:2172–2177
25. Sun Y-Y, Liao J-H, Fang J-M, Chou P-T, Shen Ch-H, Hsu Ch-W, L-Ch Chen (2006) Org Lett 8:3713–3716
26. Becke AD (1993) J Chem Phys 98:5648
27. Frisch MJ et al. (2009) Gaussian 09, Revision A.02, Gaussian, Inc., Wallingford CT
28. Hehre WJ, Ditchfield R, Pople JA (1972) J Chem Phys 56:2257
29. Miertus S, Scrocco E, Tomasi J (1981) Chem Phys 55:117
30. Tomasi J, Mennucci B, Cammi R (2005) Chem Rev 105:2999
31. Alivisatos AP, Johnsson KP, Peng X, Wilson TE, Loweth CJ, Bruchez MP, Schultz PG (1996) Nature 382:609–611
32. Daniel MC, Astruc D (2004) Chem Rev 104:293–346
33. Dooley ChJ, Rouge J, Ma N, Invernale M, Kelley SO (2007) J Mater Chem 17:1687–1691
34. Yang J, Lee JY, Too H-P, Chow G-M, Gan LM (2006) Chem Phys 323:304–312
35. Hill HD, Hurst SJ, Mirkin ChA (2009) Nano Lett 9:317–321
36. Zhao W, Brook MA, Li YF (2008) Chembiochem 9:2363–2371
37. Zhao WA, Chiuman W, Lam JFC, McManus SA, Chen W, Cui YG, Pelton R, Brook MA, Li YF (2008) J Am Chem Soc 130:3610–3618
38. Hinds S, Taft BJ, Levina L, Sukhovatkin V, Dooley CJ, Roy MD, MacNeil DD, Sargent EH, Kelly SO (2006) J Am Chem Soc Comm 128:64–65
39. Cywinski PJ, Moro AJ, Stanca SE, Biskup Ch, Mohr GJ (2009) Sens Actuators B Chem B135:472–477
40. Lapresta-Fernandez A, Cywinski PJ, Moro AJ, Mohr GJ (2009) Anal Bioanal Chem 395:1821–1830
41. McLaurin EJ, Greytak AB, Bawendi MG, Nocera DG (2009) J Am Chem Soc 131:12994–13001
42. Borisov SM, Krause Ch, Arain S, Wolfbeis OS (2006) Adv Mater 18:1511–1516
43. Lakowicz JR (2006) Principles of fluorescence spectroscopy, 3rd edn. Springer, Heidelberg
44. Seidel CAM, Schulz A, Sauer MHM (1996) J Phys Chem 100:5541–5553
45. Zhao Z, Yang J, Wu X, Su B, Sun Ch, Liu S (2004) Anal Bioanal Chem 380:104–107
46. Cywinski PJ, Idzik RI, Cranfield CG, Beckert R, Mohr GJ (2010) Supramol Chem 22:598–602